3.7–3.8 (m, 1 H), 2.2 (d, J = 5 Hz, OH, 1 H), 2.1 (s, 3 H), 1.2–1.5 (m, 4 H), 0.9 ppm (bt, J = 6 Hz, 3 H); ^{13}C NMR 171.50, 69.82, 68.69, 32.82, 27.31, 22.40, 20.68, 13.73 ppm. Anal. Calcd for $C_8H_{16}O_3$: C, 59.95; H, 10.17. Found: C, 59.87; H, 9.8.

1-(Benzyloxy)hexan-2-ol (24): oil, yield 65 mg (52%); ^{1}H NMR 7.3 (bs, 5 H), 4.5 (s, 2 H), 3.8 (m, 1 H), 3.5 (dd, J = 3.5, 8 Hz, 1 H), 3.3 (dd, J = 8, 8.8 Hz, 1 H), 2.3 (d, J = 4 Hz, OH, 1 H), 1.2–1.6 (m, 4 H), 0.9 ppm (bt, J = 6 Hz, 3 H); ^{13}C NMR 138.19, 128.69, 128.60, 128.03, 127.86, 74.65, 73.31, 70.42, 32.68, 27.51, 22.54, 13.78 ppm. Anal. Calcd for $C_{13}H_{20}O_2$: C, 74.94; H, 9.68. Found: C, 74.82; H, 9.66.

1-[(*tert*-Butyldimethylsilyl)oxy]hexan-2-ol (25): oil; yield 103 mg (78%); ^{1}H NMR 3.6 (m, 2 H), 3.3–3.4 (dd, J = 9, 10 Hz, 1 H), 2.45 (d, J = 3.3 Hz, OH, 1 H), 1.2–1.4 (m, 4 H), 0.9 (s, 12 H), 0.1 ppm (s, 6 H); ^{13}C NMR 71.78, 67.23, 32.32, 27.58, 25.70, 22.59, 18.08, 13.80, -5.62 ppm. Anal. Calcd for $C_{13}H_{28}O_2$: C, 72.15; H, 13.05. Found: C, 72.01; H, 13.0.

(6*Z*)-1-(Benzyloxy)-6-nonen-2-ol (28): oil; yield 30 mg (85%); ^{1}H NMR 7.3 (bs, 5 H), 5.2–5.4 (m, 2 H), 4.5 (s, 2 H), 3.8 (m, 1 H), 3.4–3.5 (m, 1 H), 3.2–3.3 (m, 1 H), 2.3 (d, J = 3.5 Hz, OH, 1 H), 2.0 (m, 2 H), 1.4 (m, 2 H), 0.9 ppm (t, J = 7.1 Hz, 3 H); ^{13}C NMR 132.17, 128.81, 128.59, 127.91, 127.86, 74.58, 73.31, 70.31, 32.49, 26.22, 25.43, 20.33, 14.15 ppm. Anal. Calcd for $C_{16}H_{24}O_2$: C, 77.36; H, 9.74. Found: C, 77.31; H, 9.76.

3,8-Dimethyl-7-nonene-1,2-diol (29): oil; mixture of diastereoisomers (erythro/threo (2/1)), yield 156 mg (50%); ^{1}H NMR 5.0–5.1 (m, 1 H), 3.4–3.8 (m, 3 H), 1.7–2.1 (m, 2 H), 1.65 (s, 3 H), 1.55 (s, 3 H), 1.6–1.1 (m, 5 H), 1.35 (s, OH, 1 H), 1.1 (s, OH, 1 H), 0.87 ppm (dd, J = 6.4 Hz, 3 H). Anal. Calcd for $C_{11}H_{22}O_2$: C, 70.90; H, 11.90. Found: C, 70.68; H, 11.97.

(2*S*)-5-[(*tert*-Butyldimethylsilyl)oxy]pentane-1,2-diol (30): oil; mixture of regioisomers, yield 18 mg (55%); ^{1}H NMR 3.2–4.0 (m, 5 H), 2.9 (bs, OH, 1 H), 1.4–2.1 (m, 4 H), 0.9 (s, 9 H), 0.1 ppm (s, 6 H). Anal. Calcd for $C_{12}H_{26}O_3$: C, 65.99; H, 12.00. Found: C, 65.81; H, 12.21.

(2*R*,3*S*,6*Z*)-3-(Benzoyloxy)-6-nonen-2-ol (31): oil; yield, 19 mg (85%); ^{1}H NMR 8.1 (m, 2 H), 7.2–7.6 (m, 3 H), 5.2–5.6 (m, 2 H), 5.0–5.2 (m, 1 H), 4.7 (d, J = 6.2 Hz, OH, 1 H), 3.9–4.1 (m, 1 H), 1.7–2.2 (m, 6 H), 1.2 (d, J = 6.6 Hz, 3 H), 0.9 ppm (t, J = 7.5 Hz, 3 H). Anal. Calcd for $C_{16}H_{22}O_3$: C, 73.24; H, 8.45. Found: C, 73.49; H, 8.98.

5-Hexene-2,3-diol (32): oil; mixture of diastereoisomers, yield 106 mg (85%); ^{1}H NMR 5.8–6.0 (m, 1 H), 5.1–5.35 (m, 2 H), 3.8–4.2 (m, 2 H), 1.7–2.1 (m, 2 H), 2.0 (bs, OH, 2 H), 1.2 (d, J = 6.5 Hz, 3 H). Anal. Calcd for $C_6H_{12}O_2$: C, 62.02; H, 10.42. Found: C, 61.89; H, 10.63.

Acknowledgment. This work was partially supported by a MURST grant and by C.N.R. Progetto Finalizzato "Chimica Fine e Secondaria".

Supplementary Material Available: ^{1}H and ^{13}C NMR spectra for all listed compounds (32 pages). Ordering information is given on any current masthead page.

Ab Initio Theoretical Studies on the Homotrimethylenemethane (HTMM) Diradical and Two Monomethyl-Substituted Derivatives

Daniel J. Pasto* and Derrick C. Benn

Department of Chemistry and Biochemistry, University of Notre Dame, Notre Dame, Indiana 46556

Received May 7, 1991

Ab initio calcuations have been carried out on the singlet and triplet states of the lowest energy conformation of the homotrimethylenemethane diradical **28** (HTMM) at the CASSCF, 4-31G level with full geometry optimization. At this level the lowest energy triplet state is only 0.77 kcal/mol^{-1} lower in energy than the singlet state, and the geometries are essentially identical, indicating that there is no interaction between the two radical centers in the intermediate. Geometry optimization calculations at the UHF 6-31G* level on the HTMM energy surface have located two other minimum-energy conformations **31** and **29** lying 0.56 and 1.61 kcal mol^{-1} higher in energy. Optimization calculations at the 6-31G* level indicate that the energy barriers for rotation about the C_1–C_2 and C_1–C_9 bonds in **28** are approximately 1.68 and 1.62 kcal mol^{-1}, respectively. The effect of the values of these energy barriers on the stereochemistry of the (2 + 2) cycloaddition reactions of optically active 1,3-dimethylallene are discussed. Calculations have been also carried out on the methyl-substituted HTMM's **24** and **25** at the 4-31G level as models for the substituted diradical intermediates formed in the (2 + 2) cycloaddition reactions of substituted allenes with variously substituted radicophiles, and rotational energy barriers for racemization processes in the diradical intermediates have been estimated. The results of these calculations are compared with the proposed structures of substituted HTMM's formed in the (2 + 2) cycloaddition reactions of substituted allenes and in the methylenecyclobutane rearrangement.

Introduction

Substituted homotrimethylenemethane diradicals (HTMM's, **1**) have been implicated as intermediates in the thermal rearrangement of methylenecyclobutanes[1] and as intermediates in the (2 + 2) cycloaddition reactions of substituted allenes. Several different conformations have been proposed for the substituted HTMM's formed in the rearrangement and (2 + 2) cycloaddition reactions.

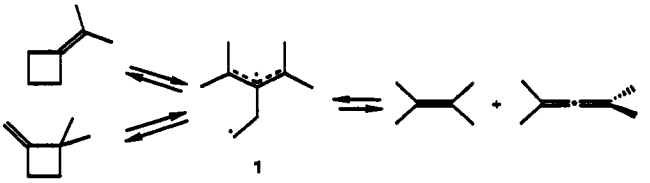

1

Doering and Gilbert reported on the kinetics of the thermal equilibrium of **2** and **3** and suggested that in view of the fact that the observed activation energy exceeded the expected bond dissociation energy of the distal C_2–C_3 or C_3–C_4 bond the rearrangement proceeded via a diradical

(1) For a review see: Gajewski, J. J. *Hydrocarbon Thermal Isomerizations*, Academic Press, New York, 1981; pp 90–94.

0022-3263/91/1956-6209$02.50/0

intermediate whose structure was represented as 4.[2]

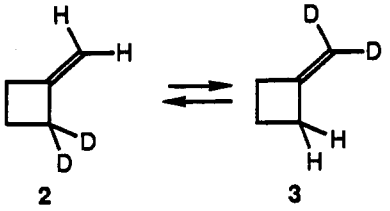

2 3

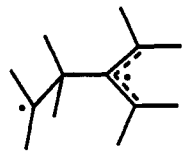

4

The results of studies by Baldwin and Fleming have shown that optically active 2-methylmethylenecyclobutane (5, 6) undergoes racemization faster than it is converted to ethylidenecyclobutane (7).[3] However, optically active (Z)-2-methylethylidenecyclobutane (8, 9, R = H) racemizes more slowly than (Z)-2-methyl(1-deuterioethylidene)-cyclobutane (8, 9, R = D) equilibrates with (Z)-2-deuterio-2-methylethylidenecyclobutane (10).[4] It was concluded that "at least some of the 1,3-carbon migration occurs with antarafacial allylic participation."[4] The results of studies on more complex deuterium-labeled systems were interpreted in support of this view.[3] Diradical intermediates were not invoked as possible intermediates.

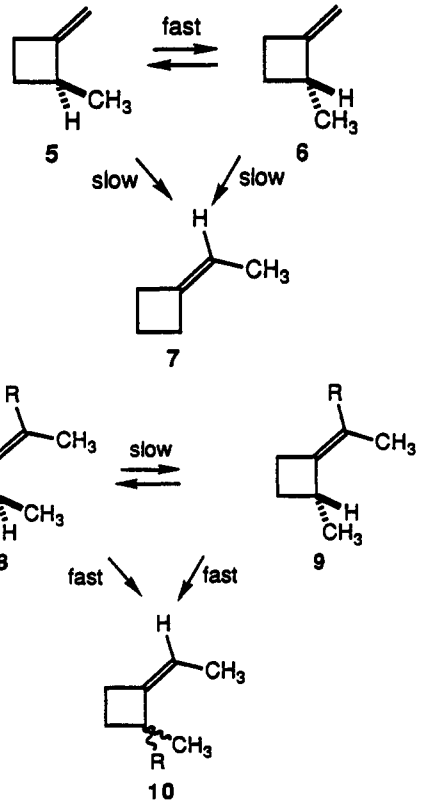

5 6 7 8 9 10

A detailed reevaluation of the earlier reported kinetic and stereochemical results led Gajewski to propose that the rearrangement of the 2-methylmethylene- and 2-methylethylidenecyclobutanes occurs via a ring-opening pathway involving conrotatory, bevel opening with outward rotation of the methyl group to form a diradical intermediate formulated as 12 derived from the optically active 11.[5] Intermediate 12 is proposed to undergo a least-motion ring closure roughly one-third of the time, with its major fate being rotation about the C_3–C_4 bond (along with possible rotation about the C_1–C_4 bond) to produce 13, which undergoes ring closure in random fashion.[5]

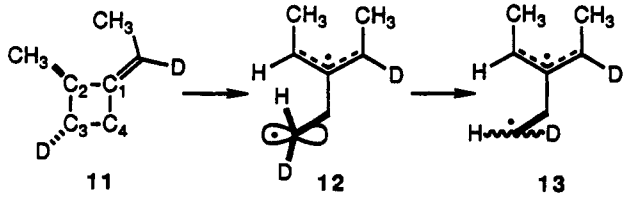

11 12 13

In 1969, Baldwin and Roy suggested the formation of the asymmetric diradical intermediates 14 and 15 as intermediates in the cycloaddition reaction of (R)-(−)-1,3-dimethylallene with acrylonitrile, which produces four optically active (2 + 2) cycloadducts possessing the R configuration at the methyl-bearing ring carbon atom.[6] In the proposed diradical intermediates 14 and 15 the C_1–C_9 bond is oriented perpendicular to the plane of the allyl radical portion of the intermediates with the H and CN groups at the aliphatic radical center oriented as shown.[6] The authors suggested that ring closure occurred more rapidly than rotation about the C–C bonds in the alkyl-radical portion of the intermediates, thus preserving optical activity in the cycloadducts. Recent studies in our laboratories have indicated that in addition to the formation of diradical intermediates having the anti,syn stereochemistry present in 14 and 15 diradical intermediates are also formed having the anti,anti stereochemistry shown in 16.[7]

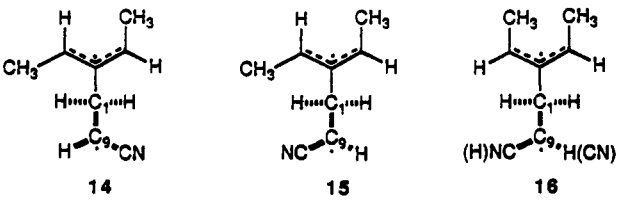

14 15 16

A detailed analysis of the distribution of the stereoisomeric cycloadducts derived from the cycloaddition reactions of alkyl-subtituted allenes with diethyl fumarate led Pasto and Yang to suggest in 1984 that the diradical intermediates formed in these cycloaddition reactions exist primarily in the conformations shown in 17 in which the largest group attached to C_1 was oriented perpendicular to the plane of the allyl radical.[8]

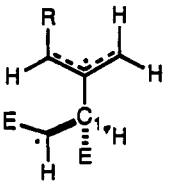

17 (R = $CO_2C_2H_5$)

In 1985, Dolbier and Wicks suggested the formation of two kinetically distinguishable diradical intermediates 18 and 19 in order to account for the distribution of the cycloadducts formed in the cycloaddition reaction of styrene with 1,1-difluoroallene.[9]

(2) Doering, W. v. E.; Gilbert, J. C. *Tetrahedron Suppl.* **1966**, *7*, 387. Chesick, J. P. *J. Phys. Chem.* **1961**, 465, 2170.
(3) Baldwin, J. E.; Fleming, R. H. *J. Am. Soc.* **1973**, *95*, 5256.
(4) Baldwin, J. E.; Fleming, R. H. *J. Am. Chem. Soc.* **1973**, *95*, 5261.
(5) Gajewski, J. J. *J. Am. Chem. Soc.* **1976**, *98*, 5254.
(6) Baldwin, J. E.; Roy, U. V. *J. Chem. Soc. D* **1969**, 1225.
(7) Pasto, D. J.; Sugi, K. D. *J. Org. Chem.* **1991**, *56*, 3781.
(8) Pasto, D. J.; Yang, S.-H. *J. Am. Chem. Soc.* **1984**, *106*, 152.
(9) Dolbier, Jr.; W. R.; Wicks, G. E. *J. Am. Chem. Soc.* **1985**, *107*, 3626.

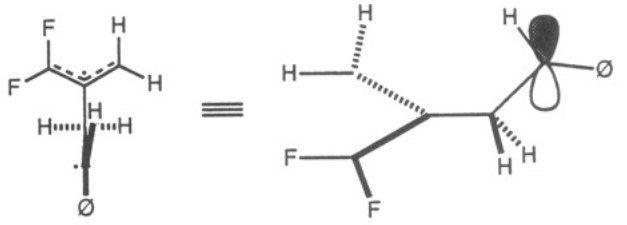

18

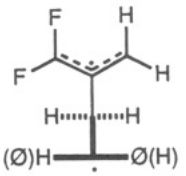

19

There appears to have been very little theoretical attention paid to HTMM system in contrast to the extensive attention given to the closely related singlet and triplet states of trimethylenemethane[10] (**20s** and **20t**) and tetramethylene[11] (**21**) diradicals. A recent publication by

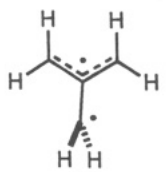

20s

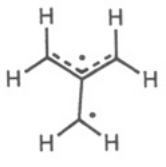

20t

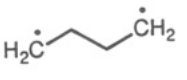

21

Skancke and co-workers[12] described the results of some ab initio calculations on HTMM carried out at the 3-21G level. Calculations were carried out on the "lowest singlet states" **22** and **23**, which were "completely optimized with analytical first and second derivatives". However, the authors later state "analytically calculated vibrational frequencies in the UHF approximation using the 3-21G basis at the C_s-constrained optimized geometries gave one imaginary frequency for each species" and thus do not represent true minimum-energy structures. The complete energy surface of the parent HTMM apparently was not explored.

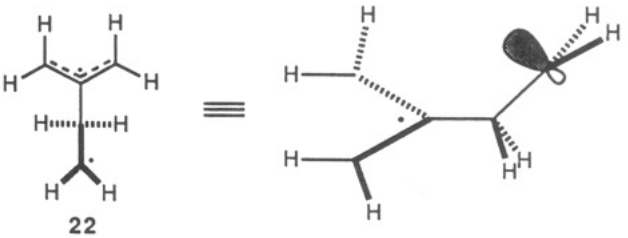

22

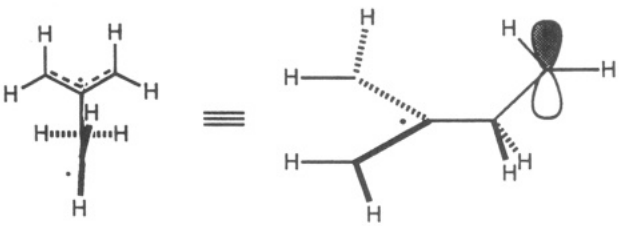

23

The great variety of conformations proposed for the structures of the diradical intermediates described above and the results derived from our current experimental studies on the stereochemical features of the cycloaddition reactions of enantioenriched 1,3-dimethylallene (13DMA) with various radicophiles has prompted a more thorough theoretical study of the parent HTMM and the two methyl-substituted derivatives **24** and **25** (as models for the anti,syn diradical intermediates formed in the cycloaddition reactions of 1,3-dimethylallene with radicophiles) in order to determine the structures of the minimum-energy conformations of HTMM, **24**, and **25** and the energy barriers for rotation about the C_1–C_2 and C_1–C_9 bonds which would result in the racemization of asymmetric intermediates.[7,13] Experimental results indicate that racemization of **26** by rotation about either the C_1–C_2 or C_1–C_9 bonds is competitive with ring closure. However, in **27**, racemization, which requires rotations about *both* the C_1–C_2 and C_1–C_9 bonds does not appear to be competitive with ring closure. The calculation of the energy barriers for rotation about the C–C bonds in HTMM, **24**, and **25** will also indirectly provide information on the relative magnitudes of the energy barriers for ring closure of these intermediates.

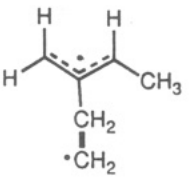

24

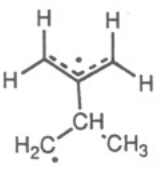

25

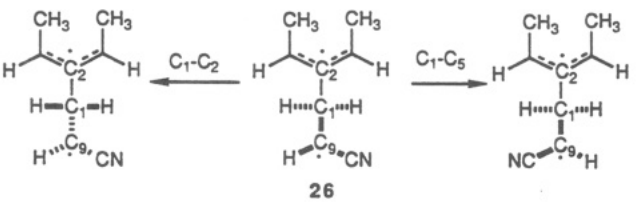

26

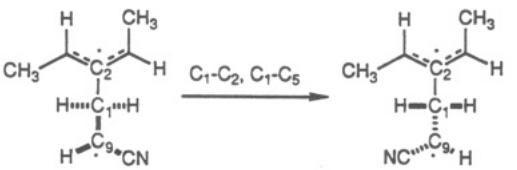

27

Results and Discussion

The initial studies on the parent HTMM were carried out on the triplet state at the UHF 4-31G level with full geometry optimization using the GAUSSIAN86[14] and -88[15] programs. After potential minimum-energy structures for HTMM were located at the 4-31G level, final geometry optimization calculations were carried out at the 6-31G* level. Vibrational analysis showed that all of the minimum-energy structures possessed zero negative force constants. The lowest energy structure located in these calculations has the geometry shown in **28**. The calculated

(10) See: Borden, W. T. Effects of Electron Repulsion in Diradicals. In Diradicals; W. T. Borden, Ed., John Wiley & Sons: New York, 1982; pp 24–36.

(11) Reference 5, pp 19–21.

(12) Skancke, P. N.; Koga, N.; Morokuma, K. *J. Am. Chem. Soc.* **1989**, *111*, 1559.

(13) Pasto, D. J.; Sugi, K. D. *J. Org. Chem.* **1991**, *56*, 3795.

(14) GAUSSIAN 86, Frisch, M. J.; Binkley, J. S.; Schlegel, H. B.; Raghavachari, K.; Melius, C. F.; Martin, L.; Stewart, J. J. P.; Bobrowicz, F. W.; Rohlfing, C. M.; Kahn, L. R.; Defrees, D. J.; Seeger, R.; Whiteside, R. A.; Fox, D. J.; Fleuder, E. M.; Pople, J. A. Carnege-Mellon Quantum Chemistry Publishing Unit, Pittsburgh, PA.

(15) GAUSSIAN 88, Frisch, M. J.; Head-Gordon, M.; Schlegel, H. B.; Raghavachari, K.; Binkley, J. S.; Gonzalez, C.; Defrees, D. J.; Fox, D. J.; Whiteside, R. A.; Seeger, R.; Milius, C. F.; Baker, J.; Martin, R. L.; Kahn, L. R.; Stewart, J. J. P.; Fluder, E. M.; Topiol, S.; Pople, J. A. GAUSSIAN, Inc., Pittsburgh, PA.

Table I. Calculated Structural Parameters for 28 at Various Levels of Computation

parameter	basis-set level[a] UHF/ 4-31G (T)	CASSCF/ 4-31G (T)	CASSCF/ 4-31G (S)	UHF/ 6-31G* (T)
	Bond Lengths			
C_1–C_2	1.525	1.527	1.529	1.524
C_2–C_3	1.392	1.391	1.391	1.395
C_2–C_4	1.392	1.391	1.391	1.395
C_1–C_9	1.504	1.503	1.503	1.505
C_3–H_5	1.073	1.072	1.072	1.075
C_4–H_6	1.073	1.072	1.072	1.075
C_3–H_7	1.073	1.072	1.072	1.075
C_4–H_8	1.073	1.072	1.072	1.075
C_1–H_{10}	1.083	1.084	1.084	1.085
C_1–H_{11}	1.083	1.084	1.084	1.085
C_9–H_{12}	1.073	1.073	1.072	1.076
C_9–H_{13}	1.073	1.073	1.072	1.076
	Bond Angles			
C_1–C_2–C_3	119.18	119.10	119.11	119.37
C_1–C_2–C_4	119.18	119.05	119.08	119.37
C_2–C_1–C_9	110.61	111.65	114.14	110.77
C_2–C_3–H_5	121.23	121.27	121.24	121.16
C_2–C_4–H_6	121.23	121.27	121.24	121.16
C_2–C_3–H_7	121.64	121.62	121.61	121.58
C_2–C_4–H_8	121.64	121.62	121.61	121.58
C_2–C_1–H_{10}	109.49	109.31	108.68	109.55
C_2–C_1–H_{11}	109.49	109.31	108.69	109.55
C_1–C_9–H_{12}	120.01	119.59	120.07	119.56
C_1–C_9–H_{13}	120.01	119.56	120.07	119.56
	Dihedral Angles			
C_9–C_1–C_2–C_3	90.00	89.95	90.04	90.00
H_{10}–C_1–C_2–C_3	−148.40	−148.28	−147.75	−148.46
H_{11}–C_1–C_2–C_3	−31.60	−31.78	−32.20	−31.54
H_{12}–C_9–C_1–C_2	80.92	78.87	80.58	78.17
H_{13}–C_9–C_1–C_2	−80.92	−78.86	−80.56	−78.17

[a] T indicates triplet state, S indicates singlet state.

Table II. Total Energies for the Diradical Structures

structure	method/basis set (state)[a]	E_{tot} (au)	$\langle S^2 \rangle$
28	UHF/4-31G (T)	−193.631 67	2.2364
	CASSCF/4-31G (T)	−193.645 66	
	CASSCF/4-13G (S)	−193.644 44	
	UHF/6-31G* (T)	−193.906 61	2.2276
29	UHF/6-31G* (T)	−193.904 05	2.2282
31	UHF/6-31G* (T)	−193.905 71	2.2284
33	UHF/4-31G (T)	−232.608 60	2.2371
34	UHF/4-31G (T)	−232.607 00	2.2417
35	UHF/4-31G (T)	−232.607 71	2.2413
36	UHF/4-31G (T)	−232.607 00	2.2380
37	UHF/4-31G (T)	−232.608 74	2.2417
38	UHF/4-31G (T)	−232.607 07	2.2421

[a] T indicates triplet state, S indicates singlet state.

structural parameters are given in Table I, and the total energy is given in Table II. Note that the geometry at C_9 is inverted relative to that shown in **22**.[12] No evidence could be found at the 6-31G* level for the existence of any minimum-energy structure corresponding to that shown in **22**. Starting with a configuration at the aliphatic radical center as shown in **22** results in a smooth inversion to **28**. The radical center at C_9 is quite pyramidalized and is consistent with the extent of pyramidalization observed in simple alkyl radicals such as the propyl radical.[16] The pyramidalization of the radical center arises from the mixing of the singly occupied orbital at C_9 with the C_1–C_2 σ^* MO.

Ab initio calculations have been carried out on the singlet state of **28** using the GAMESS package programs.[17]

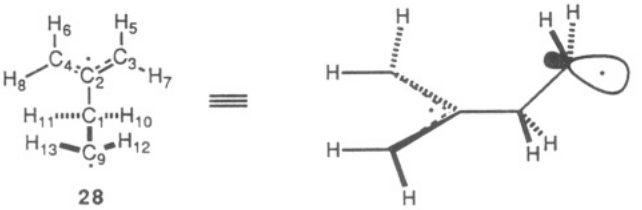

28

Initial calculations on the singlet state carried out using the GVB method indicated that this method suffered from symmetry instability problems in dealing with the allyl radical portion of **28**. Calculation of the UHF natural orbitals[18] indicated an extensive transfer of electron density from the bonding π-allyl MO (MO no. 18) to the antibonding π-allyl MO (MO no. 21). (The occupation numbers for MO's 18–21 are calculated to be 1.8853, 1.0000, 1.0000, and 0.1147, respectively.) Accordingly, CASSCF calculations were carried out on both the singlet and triplet states of **28** at the 4-31G level with full geometry optimization using the GAMESS program. These calculations involved 20 configurations for the singlet state and 15 configurations for the triplet state for the four electrons in the three π-allyl orbitals and the single aliphatic radical orbital. Again, vibrational analysis at the CASSCF level indicated zero negative force constants. The CASSCF-optimized structural parameters for the singlet and triplet states of **28** are very similar (see Table I) and are very similar to the calculated structural parameters derived at the UHF 4-31G level. At the CASSCF geometry optimized level the triplet state is calculated to be lower in energy by only 0.77 kcal mol^{-1} (see Table II). The very close similarity in the CASSCF-optimized geometries and total energies of the triplet and singlet states indicates that there is *no* interaction between the allyl (a″) and alkyl (a′) radical centers and that the calculationally simpler UHF triplet calculations will provide an adequate description of the singlet state of **14** and its derivatives. It must be noted that the symmetry of the two SOMO's are different and are not expected to mix, which would result in a substantial singlet–triplet energy gap. The same will hold true for the other two minimum-energy conformations of HTMM which were located.

Starting with the perpendicular optimized structure **28**, a potential energy surface scan was carried out for rotation about the C_1–C_2 bond, maintaining the optimized geometrical parameters calculated for **28**, proceeding to the all-planar carbon framework of **29** (see Figure 1). (The continuation of this process would result in the racemization of an appropriately substituted chiral HTMM as described earlier in the case of **26**.) There is no inflection point in this plot that would suggest that a conformation having the C_1–H_{10} bond perpendicular to the allyl radical portion of the intermediate might represent a local minimum-energy structure. Geometry optimization of the planar conformation **29** at the 6-31G* level results in a minimum-energy structure having the configuration at the radical center shown in **29**, again with the radical center oriented antiperiplanar to the C_1–C_2 bond as in **28**. (The calculated structural parameters are given in Table III and the total energy is given in Table II.) This is a true minimum-energy conformation as indicated by starting the optimization from a slightly nonplanar, non-C_s structure, the optimization returning to the C_s structure and possessing no negative force constants. A structure with the inverted configuration at the radical center again does not

(16) Pecansky, J.; Dupuis, M. *J. Chem. Phys.* **1980**, *71*, 2095.

(17) GAMESS, Dupuis, M.; Spangler, D.; Wendoloski, J. J. National Resources for Computations in Chemistry, Berkeley, CA.

(18) Pulay, P.; Hamilton, T. P. *J. Chem. Phys.* **1988**, *88*, 4926.

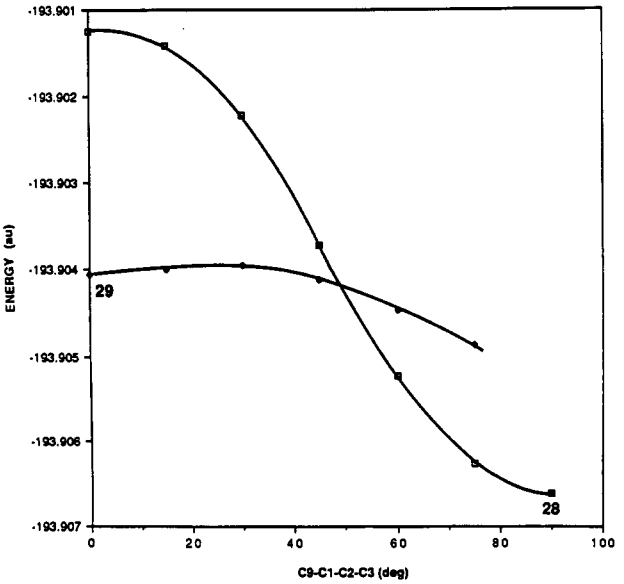

Figure 1. 6-31G* potential energy surface scan about the C_9–C_1–C_2–C_3 dihedral angle starting from the optimized structure of **28** (90°) toward **29** (0°) and starting from the optimized structure for **29** (0°) toward **28**.

Table III. Calculated Structural Parameters for 29 and 31 at the 6-31G* Level

parameter	29	31
	Bond Lengths	
C_1–C_2	1.530	1.523
C_2–C_3	1.388	1.391
C_2–C_4	1.399	1.397
C_1–C_9	1.502	1.502
C_3–H_5	1.075	1.075
C_4–H_6	1.073	1.075
C_3–H_7	1.075	1.075
C_4–H_8	1.075	1.075
C_1–H_{10}	1.087	1.088
C_1–H_{11}	1.087	1.090
C_9–H_{12}	1.075	1.076
C_9–H_{13}	1.075	1.075
	Bond Angles	
C_1–C_2–C_3	121.84	119.67
C_1–C_2–C_4	117.40	119.29
C_2–C_3–H_5	120.51	121.11
C_2–C_3–H_7	122.22	121.75
C_2–C_4–H_6	121.17	120.94
C_2–C_4–H_8	121.52	121.54
C_2–C_1–H_{10}	108.01	109.15
C_2–C_1–H_{11}	108.01	108.91
C_1–C_9–H_{12}	120.65	119.82
C_1–C_9–H_{13}	120.65	120.21
	Dihedral Angles	
C_9–C_1–C_2–C_3	0.00	125.85
H_{10}–C_1–C_2–C_3	122.90	2.96
H_{11}–C_1–C_2–C_3	-122.90	-11.85
H_{12}–C_9–C_1–C_2	83.48	-198.10
H_{13}–C_9–C_1–C_2	-83.48	35.75

represent a minimum-energy structure. The potential energy well of **29**, however, is very shallow as is indicated by the potential energy surface scan for rotation about the C_1–C_2 bond, while maintaining the other geometrical parameters of **29** constant, from **29** toward **28**. On leaving **29** toward **28** there is a slight rise in total energy representing an energy barrier for going from **29** to **28**, or the enantiomer of **28**, estimated to be of the order of only ~0.1 kcal mol^{-1}. Because of the very flat nature of the energy surface in the region of the transition state for the conversion of **29** to **28**, no attempt was made to try to locate the transition state. The energy barrier for racemization

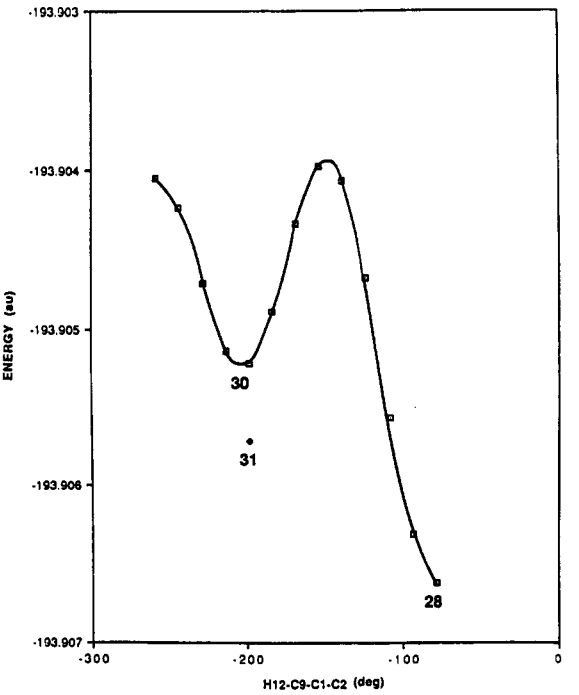

Figure 2. 6-31G* potential energy surface scan about the H_{12}–C_9–C_1–C_2 dihedral angle starting from the optimized structure of **28**. The black diamond at ~200° is the energy of the optimized structure **31**.

of **28** by a 180° rotation about the C_1–C_2 bond is estimated to be 1.68 kcal mol^{-1} at the 6-31G* level, which should be a lower limit for the energy barriers for the racemization of chiral anti,anti diradical intermediates such as **26**.

A potential energy surface scan was also carried out for rotation about the C_1–C_9 bond in **28** holding the remainder of the geometrical parameters of **28** constant (see Figure 2). (This mode of rotation also provides a route for racemization of certain substituted chiral HTMM's such as **26** as described earlier.) This scan indicated the possibility of a minimum-energy structure **30** in which the radical center is antiperiplanar to the C_1–H_{10} bond. However, optimization in this region resulted in a slow twisting about the C_1–C_2 bond ultimately leading to the structure **31** in which the C_1–H_{11} bond is essentially eclipsed with the C_2–C_3 bond of the allyl radical (see Tables II and III for the calculated structural parameters and total energy). This structure resembles that shown in **12** which might actually be a true energy-minimum intermediate formed in the rearrangement of **11**. With the apparent complexity of the structures and the relative flatness of the energy surface for rotation about the C_1–C_2 bond during the optimization of **31**, the location of the transition state for the conversion of **28** to **31** was not attempted. The geometry near the transition state for this rotation resembles the geometry proposed for intermediate **18**. The Mulliken population analysis indicates that there is essentially no long-range interaction between the 2p AO of the SOMO with the 2p AO's of the allyl radical portion of the intermediate. The minimum energy barrier for rotation about the C_1–C_9 bond, which would result in the racemization of an appropriately substituted chiral HTMM such as **26**, is estimated to be 1.62 kcal mol^{-1}.

In summary, the results of the UHF 6-31G* optimization calculations on the parent HTMM have located three minimum-energy conformations; **28** being the lowest in energy, with **31** being 0.56 kcal mol^{-1} higher in energy and **29** 1.61 kcal mol^{-1} higher in energy. In addition, estimates for the energy barriers for rotation about the C_1–C_2 and

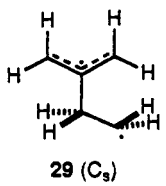

29 (C_s)

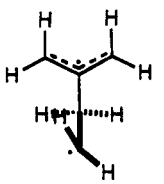

30

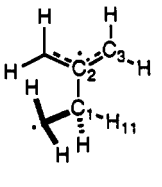

31

C_1–C_9 bonds, which would result in the racemization of chiral anti,anti diradical intermediates, have been obtained that would appear to be similar in magnitude with the energy barriers for ring closure as evidenced by the results of stereochemical studies carried out in our laboratories.[7]

Theoretical Studies on the Monomethyl-Substituted HTMM's 24 and 25. Geometry-optimization calculations carried out at the UHF 4-31G level on **24** starting from a perpendicular conformation resulted in slow optimization to **32** in which the C_8–H_9 bond is eclipsed with the C_2–C_4 bond and the C_1–C_{11} bond is slightly out of being perpendicular to the plane of the allyl radical portion of the intermediate (C_{11}–C_1–C_2–C_3 dihedral angle of 95.02°). (The calculated structural parameters are shown in the structure and the total energy is given in Table II.) Again, the radical center is oriented antiperpiplanar to the C_1–C_2 bond. (Other minimum-energy conformations about the C_1–C_{11} bond were not searched for.) The potential energy surface scan for a 360° rotation about the C_1–C_2 bond starting from the optimized C_{12}–C_1–C_2–C_3 dihedral angle of 95.02° while maintaining the optimized geometrical parameters of **32** is shown in Figure 3. The nonoptimized energy barrier for rotation of the $-CH_2^{\bullet}$ group past the methyl group is 5.68 kcal mol^{-1}. The minimum-energy point near 265° represents the mirror-image structure of **32**. The maximum in the region of ~320° represents the passage of the C_1–H_{10} past the methyl group along with an increasing repulsive interaction developing between the $-CH_2^{\bullet}$ and the C_3–H_7 bond. The maximum at ~360° represents an eclipsed conformation between the $-CH_2^{\bullet}$ and C_3–H_7 bond along with some residual interaction between the C_1–H_{10} and the methyl group. The calculated energy barrier for rotation in the 320–360° dihedral angle region is ~2.86 kcal mol^{-1}. Geometry optimizations at the energy maxima have not been attempted, which would undoubtedly lower the magnitudes of the energy barriers somewhat. However, these values cannot be too far off in view of the fact that the results of experimental stereochemical studies in our laboratories suggest that the energy barriers for racemization of chiral anti,syn diradical intermediates by a 180° rotation about the C_1–C_2 bond in either direction appear to be significantly greater than the energy barriers for ring closure.

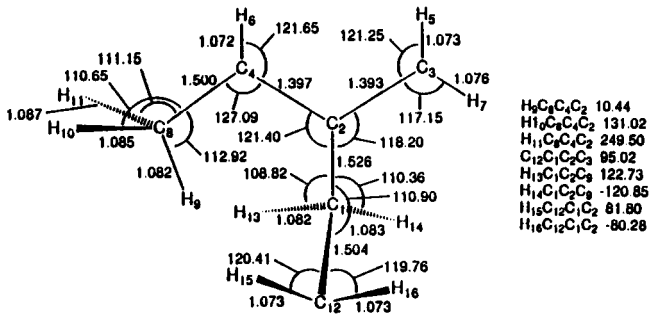

32

Geometry-optimization calculations on **25** resulted in the location of a minimum-energy conformation having the structure shown as **33** in Scheme I (see Table IV for the

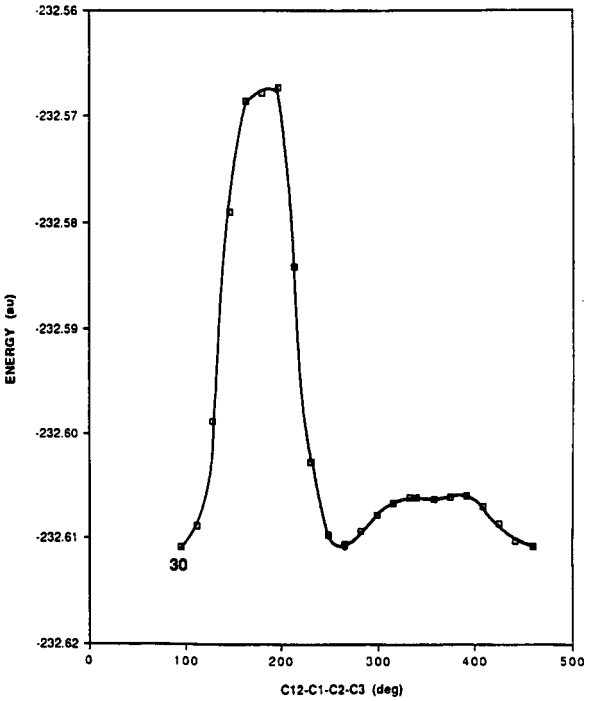

Figure 3. 4-31G potential energy surface scan about the C_{12}–C_1–C_2–C_3 dihedral angle starting from the optimized structure of **30**.

Table IV. 4-31G Optimized Structural Parameters for 33, 35, and 37

parameter	structure 33	35	37
Bond Lengths			
C_1–C_2	1.531	1.529	1.529
C_2–C_3	1.391	1.390	1.391
C_2–C_4	1.396	1.395	1.394
C_1–C_9	1.507	1.506	1.504
C_1–C_{11}	1.535	1.544	1.540
C_3–H_5	1.073	1.073	1.073
C_3–H_7	1.072	1.072	1.072
C_4–H_6	1.073	1.073	1.073
C_4–H_8	1.072	1.072	1.072
C_1–H_{10}	1.085	1.086	1.090
C_9–H_{15}	1.074	1.074	1.073
C_9–H_{16}	1.073	1.072	1.074
C_{11}–H_{12}	1.083	1.084	1.084
C_{11}–H_{13}	1.083	1.082	1.083
C_{11}–H_{14}	1.083	1.083	1.082
Bond Angles			
C_1–C_2–C_3	119.12	119.20	119.02
C_1–C_2–C_4	119.89	119.74	119.70
C_2–C_3–H_5	121.15	121.16	121.21
C_2–C_3–H_7	121.73	121.74	121.70
C_2–C_4–H_6	120.91	120.94	121.02
C_2–C_4–H_8	122.14	122.14	121.70
C_2–C_1–C_9	110.21	111.75	112.59
C_2–C_1–C_{11}	112.06	111.59	110.64
C_2–C_1–H_{10}	107.08	107.23	107.02
C_1–C_9–H_{15}	120.13	120.18	120.49
C_1–C_9–H_{16}	120.07	121.16	120.16
C_1–C_{11}–H_{12}	110.36	110.49	110.64
C_1–C_{11}–H_{13}	111.33	111.22	110.73
C_1–C_{11}–H_{14}	110.84	110.60	110.69
Dihedral Angles			
C_9–C_1–C_2–C_3	114.60	116.38	134.57
H_{10}–C_1–C_2–C_3	−2.53	−1.48	15.97
C_{11}–C_1–C_2–C_3	−120.28	−118.08	−100.40
H_{12}–C_{11}–C_1–C_2	175.91	175.96	177.37
H_{13}–C_{11}–C_1–C_2	−64.37	−64.27	−62.67
H_{14}–C_{11}–C_1–C_2	55.81	56.03	57.29
H_{15}–C_9–C_1–C_2	84.51	203.89	323.09
H_{16}–C_9–C_1–C_2	−78.10	−172.75	−167.07

Scheme I

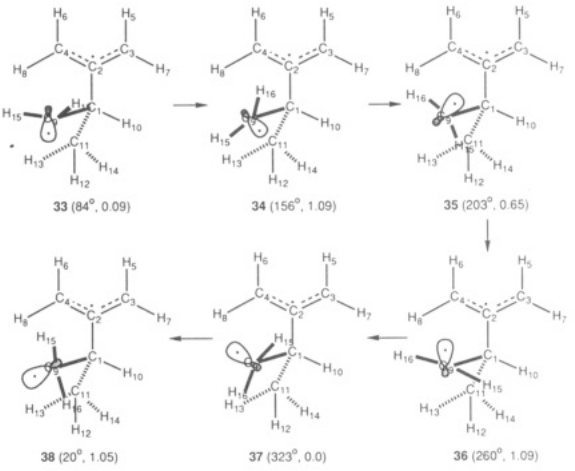

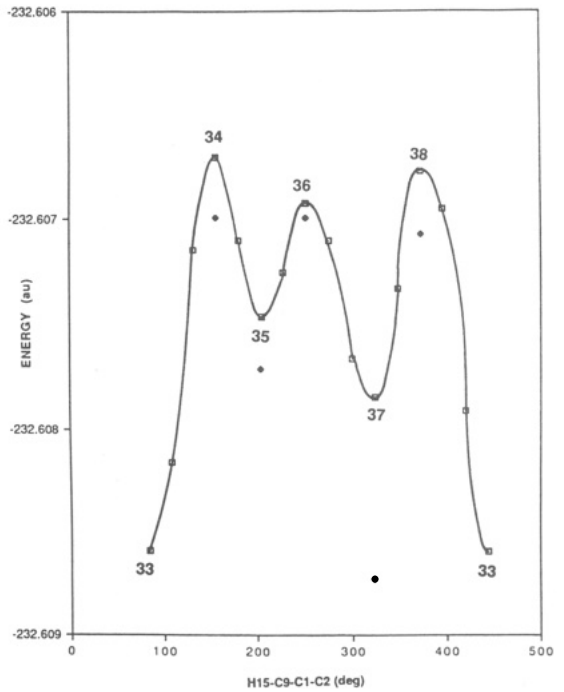

Figure 4. 4-31G potential energy surface scan about the H_{15}–C_9–C_1–C_2 dihedral angle starting from the optimized structure of **33**. The black diamonds indicate the total energies of the fully geometry-optimized structures at those dihedral angles.

calculated structural parameters for **33** and Table II for the total energy). A potential energy surface scan for rotation about the C_9–C_1 bond in **33** while maintaining the optimized geometrical parameters for **33** produced the energy plot shown in Figure 4. Geometry-optimization calculations were carried out at the 4-31G level on the maximum-energy conformations while holding H_{15}–C_9–C_1–C_2 and H_{15}–C_9–C_1–H_{16} dihedral angles constant, while full geometry-optimization calculations were carried out on the minimum-energy conformations. The total energies derived from these calculations are indicated by the black diamonds in Figure 4 and are given in Table II. The calculated structural paramters for the minimum-energy conformations **33**, **35**, and **37** are given in Table IV. The structures of **33**–**38** are shown in Scheme I, along with the H_{15}–C_9–C_1–C_2 dihedral angles and the relative energies in kcal mol^{-1} in parentheses.

The lowest energy conformation is **37** in which the radical center is antiperiplanar with the C_1–H_{10} bond. The next lowest energy conformation **33** has the radical center oriented antiperiplanar with the C_1–C_2 bond, while in the highest energy conformation **35** the radical center is oriented antiperiplanar to the C_1–C_{11} bond. It is interesting to note that in conformations **33** and **35** the C_1–H_{10} bonds are essentially eclipsed with the C_2–C_3 bond, with the C_1–C_{11} bonds being staggered with the C_4–H_8 bond. In the lowest energy conformation **37**, however, the H_{10}–C_1–C_2–C_3 dihedral angle is ~10° with the C_{11}–C_1–C_2–C_3 dihedral angle being ~105°. In this conformation the C_1–H_{11} bond is oriented more toward the perpendicular to the plane of the allyl radical than in **33** and **35**.

These results are consistent with the deductions of Pasto and Yang[8] on the conformational preferences of the diradical intermediates derived in the cycloaddition reactions of alkyl-substituted allenes with diethyl fumarate. However, in these diradical intermediates an ester group is present, which is larger than a methyl group, and which might be expected to cause more of a distortion toward an ester-perpendicular conformation in the intermediates.

Summary

The results of the theoretical calculations on the parent HTMM located three minimum-energy conformations **28**, **29**, and **31**. Structure **31** closely resembles the structure **12** proposed as in intermediate in the rearrangement of **11**. No evidence has been found suggesting that other conformations such as those shown in **13** and **18** represent minimum-energy structures on the energy surface of HTMM. (Structure **19** resembles **28**, and may well possess a planar radical center due to the presence of the phenyl group.) The calculated energy barriers for rotation about the C_1–C_2 and C_1–C_9 bonds are 1.68 and 1.62 kcal mol^{-1}.

Methyl substitution at C_3 (or C_4) causes little distortion from the lowest energy perpendicular conformation of **28**. The calculated rotational energy barriers for passage of the C_1–H and C_1–C bonds past the C_3-methyl group are estimated to be 2.86 and 5.86 kcal mol^{-1}. Methyl substitution at the C_1 results in a "staggerd" conformation in which the C_1–H_{10} bond is essentially eclipsed with the C_2–C_3 (C_2–C_4) bond.

Acknowledgment. We acknowledge support from the National Science Foundation for support of part of this study (NSF CHE8709725), a summer NSF Undergraduate Research supplement for the support of Derrick Benn, and the NSF funded National Center for Supercomputing Applications at the University of Illinois for computing time. We also acknowledge helpful discussions with Dr. Daniel Chipman of the Radiation Laboratory of the University of Notre Dame.

Registry No. 1, 135513-17-6; **24**, 135513-18-7; **25**, 135513-19-8.